ORIGINAL RESEARCH

Regenerative Therapy Prevents Heart Failure Progression in Dyssynchronous Nonischemic Narrow QRS Cardiomyopathy

Satsuki Yamada, MD, PhD; D. Kent Arrell, PhD; Almudena Martinez-Fernandez, PhD; Atta Behfar, MD, PhD; Garvan C. Kane, MD, PhD; Carmen M. Perez-Terzic, MD, PhD; Ruben J. Crespo-Diaz, PhD; Robert J. McDonald, MD, PhD; Saranya P. Wyles, BS; Jelena Zlatkovic-Lindor, PhD; Timothy J. Nelson, MD, PhD; Andre Terzic, MD, PhD

***Background*—**Cardiac resynchronization therapy using bi-ventricular pacing is proven effective in the management of heart failure (HF) with a wide QRS-complex. In the absence of QRS prolongation, however, device-based resynchronization is reported unsuitable. As an alternative, the present study tests a regenerative cell-based approach in the setting of narrow QRS-complex HF.

***Methods and Results*—**Progressive cardiac dyssynchrony was provoked in a chronic transgenic model of stress-triggered dilated cardiomyopathy. In contrast to rampant end-stage disease afflicting untreated cohorts, stem cell intervention early in disease, characterized by mechanical dyssynchrony and a narrow QRS-complex, aborted progressive dyssynchronous HF and prevented QRS widening. Stem cell-treated hearts acquired coordinated ventricular contraction and relaxation supporting systolic and diastolic performance. Rescue of contractile dynamics was underpinned by a halted left ventricular dilatation, limited hypertrophy, and reduced fibrosis. Reverse remodeling reflected a restored cardiomyopathic proteome, enforced at systems level through correction of the pathological molecular landscape and nullified adverse cardiac outcomes. Cell therapy of a dyssynchrony-prone cardiomyopathic cohort translated prospectively into improved exercise capacity and prolonged survivorship.

***Conclusions*—**In narrow QRS HF, a regenerative approach demonstrated functional and structural benefit, introducing the prospect of device-autonomous resynchronization therapy for refractory disease. **(*J Am Heart Assoc*. 2015;4:e001614 doi: 10.1161/JAHA.114.001614)**

Key Words: mechanical discordance • proteome • resynchronization • speckle-tracking • stem cells

Disparity in cardiac wall motion is associated with poor outcome. In this regard, cardiac resynchronization therapy (CRT), using implantable bi-ventricular pacing devices, has significantly advanced the management of chronic heart failure (HF). Morbidity and mortality benefits, after CRT implantation, have been documented for symptomatic patients that display reduced left ventricular ejection fraction and a wide QRS-complex.[1–3] However, CRT-based therapy is not recommended in patients with moderate-to-severe HF that do not display a wide QRS-complex, although on echocardiography show evidence of ventricular dyssynchrony.[4]

Mechanical discordance within a narrow QRS-complex is detected in primary cardiomyopathy with multiple etiologies[5–7] that initially spare the electrical conduction system.[8] In this setting, regional differences in tissue contraction could generate mechanical dyssynchrony autonomously from conduction block.[9] Importantly, failure in intrinsic force generation is less amenable to pacing therapy.[10] In fact, synchronization strategies for narrow QRS-complex HF are currently lacking.[11,12]

The present study tests a device-independent, stem cell-based intervention as a candidate therapy for narrow QRS-complex dyssynchronous HF. We applied induced pluripotent stem (iPS) cells, with a recognized capacity for heart repair in ischemic heart disease,[13–15] in a transgenic model of adult-onset nonischemic cardiomyopathy whereby mechanical dyssynchrony is an early marker of disease. Prospectively, biotherapy with iPS cells, administered at the time of narrow

From the Center for Regenerative Medicine, Marriott Heart Disease Research Program, Division of Cardiovascular Diseases, Departments of Medicine, Molecular Pharmacology and Experimental Therapeutics, and Medical Genetics (S.Y., D.K.A., A.M.-F., A.B., G.C.K, C.M.P.-T., R.J.C.-D., R.J.M., S.P.W., J.Z.-L., T.J.N., A.T.), Department of Physical Medicine and Rehabilitation (C.M.P.-T.), and Division of General Internal Medicine, William J. von Liebig Center for Transplantation and Clinical Regeneration (T.J.N.), Mayo Clinic, Rochester, MN.

Correspondence to: Andre Terzic, MD, PhD, Mayo Clinic, 200 First St SW, Rochester, MN 55905. E-mail: terzic.andre@mayo.edu

Accompanying Tables S1 and S2 are available at http://jaha.ahajournals.org/content/4/5/e001614/suppl/DC1

Received January 27, 2015; accepted April 15, 2015.

QRS-complex dyssynchrony, showed signs of benefit preventing progressive mechanical/electrical discordance that underlies malignant HF.

Methods

Protocols were carried out in accord with the National Institutes of Health guidelines and received approval of the Institutional Animal Care and Use Committee and Biosafety Committee at Mayo Clinic (Rochester, MN). Surgery was performed under 2% isoflurane anesthesia in conjunction with prophylactic administration of acetaminophen (100 to 300 mg/kg in drinking water, from 2 days pre- to 5 days post-surgery).

Cell Intervention in Dyssynchronous Cardiomyopathy

Male, 8- to 12-week-old, C57BL/6 wild-type (WT) mice and age-/sex-matched *Kcnj11*-null mutants (backcrossed into a C57BL/6 background) lacking the Kir6.2 protein of the cardioprotective ATP-sensitive K^+ (K_{ATP}) channel[16,17] underwent transverse aortic constriction (TAC) to impose chronic hemodynamic load.[18,19] Allogeneic iPS cells (DR-4 strain) were bioengineered using defined pluripotency-associated transcription factors, that is, OCT3/4 (octamer-binding transcription factor 3/4), SOX2 [SRY (sex determining region Y)-box 2], KLF4 (Krüppel-like factor 4), and c-MYC cDNAs, and labeled with HIV vectors carrying LacZ (pLenti6/UbC/

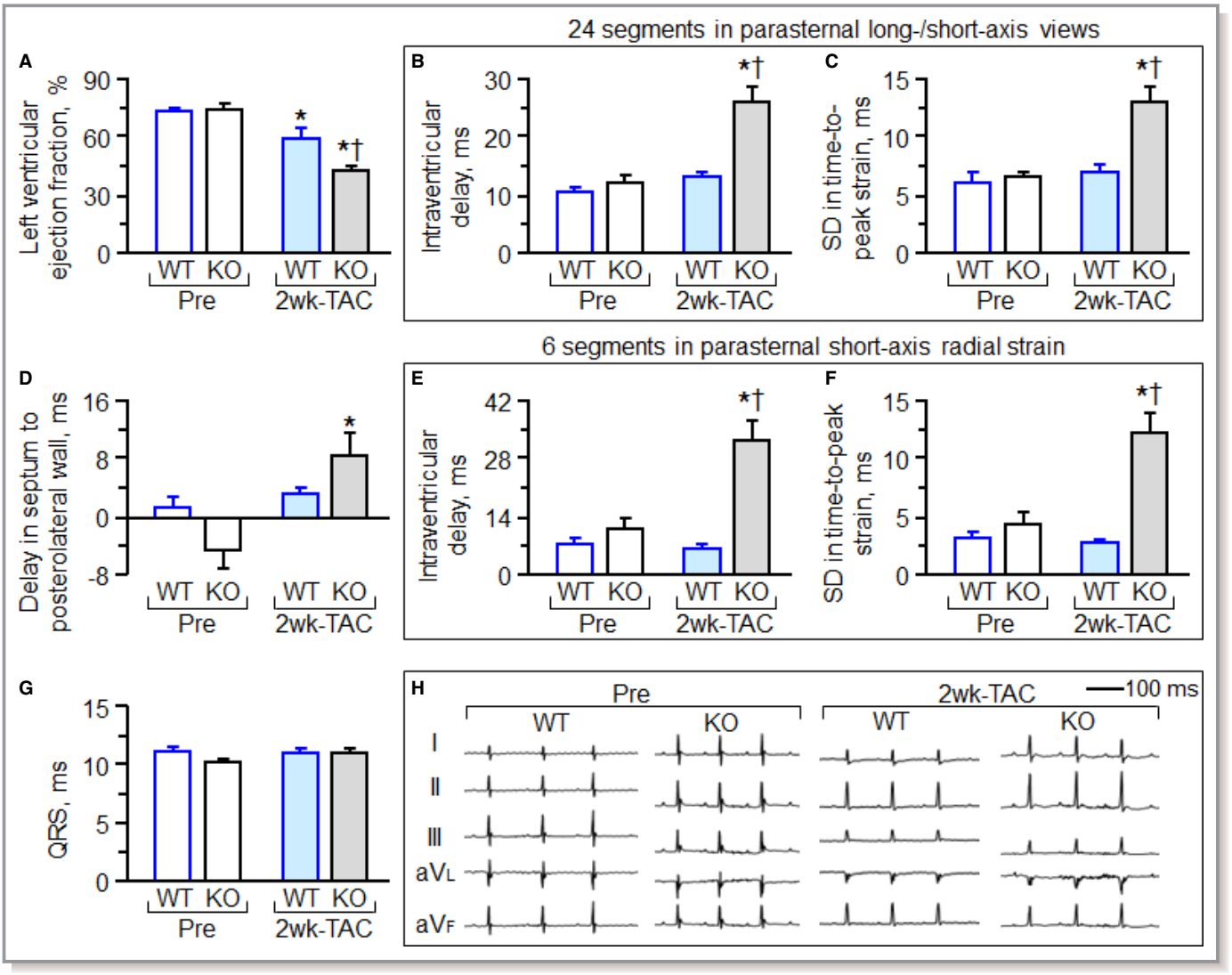

Figure 1. Mechanical dyssynchrony-prone cardiomyopathy model. Knockout of the *Kcnj11*-encoded Kir6.2 protein precipitates stress-induced cardiomyopathy with dyssynchrony. At 2 weeks post-TAC, *Kcnj11*-deficent left ventricles (KO) developed systolic dysfunction (A) with echocardiographic evidence of intraventricular delay in contractile timing (B through F), typical of mechanical dyssynchrony, in the absence of electrocardiographic change (G and H). *P<0.05 vs. Pre; †P<0.05 vs. WT 2 weeks post-TAC. KO indicates knockout; SD, standard deviation; TAC, transverse aortic constriction; WT, wild type.

V5-GW/LacZ; Invitrogen, Grand Island, NY).[20,21] In *Kcnj11*-null mice surviving at 2 weeks post-TAC, iPS cells (200 000 cells per heart in 15 μL of propagation medium) were delivered by epicardial route using a programmable microinjector (Pump 11 Elite; Harvard Apparatus, Holliston, MA) at 6 sites of the left ventricle (LV) following thoracotomy [TAC-iPS(+); n=7]. The areas of cell delivery covered the basal to apex lateral segments of the LV, where speckle-tracking echocardiography detected dyssynchronous motion characterized by severe hypokinesis with maximum delay in time-to-peak contraction.[22] In a separate cohort that did not receive iPS cells, sham [thoracotomy without cell delivery; TAC-iPS(−), n=25] treatment was implemented. The randomization ratio reflected high mortality in TAC-stressed, *Kcnj11*-null mutants assigned to the sham regimen (mortality post-TAC, 75% at 2 weeks, 85% to 90% at 3 months). Prospective follow-up for 3 months post-TAC was implemented in an investigator-blinded fashion.

In Vivo Evaluation of Cardiac Function and Structure

Cardiac function and structure were quantified in vivo by 2-dimensional (2D)/M-mode/speckle-tracking echocardiography with a 30-MHz transducer (MS-400; Vevo2100; FUJIFILM VisualSonics, Toronto, Ontario, Canada), and

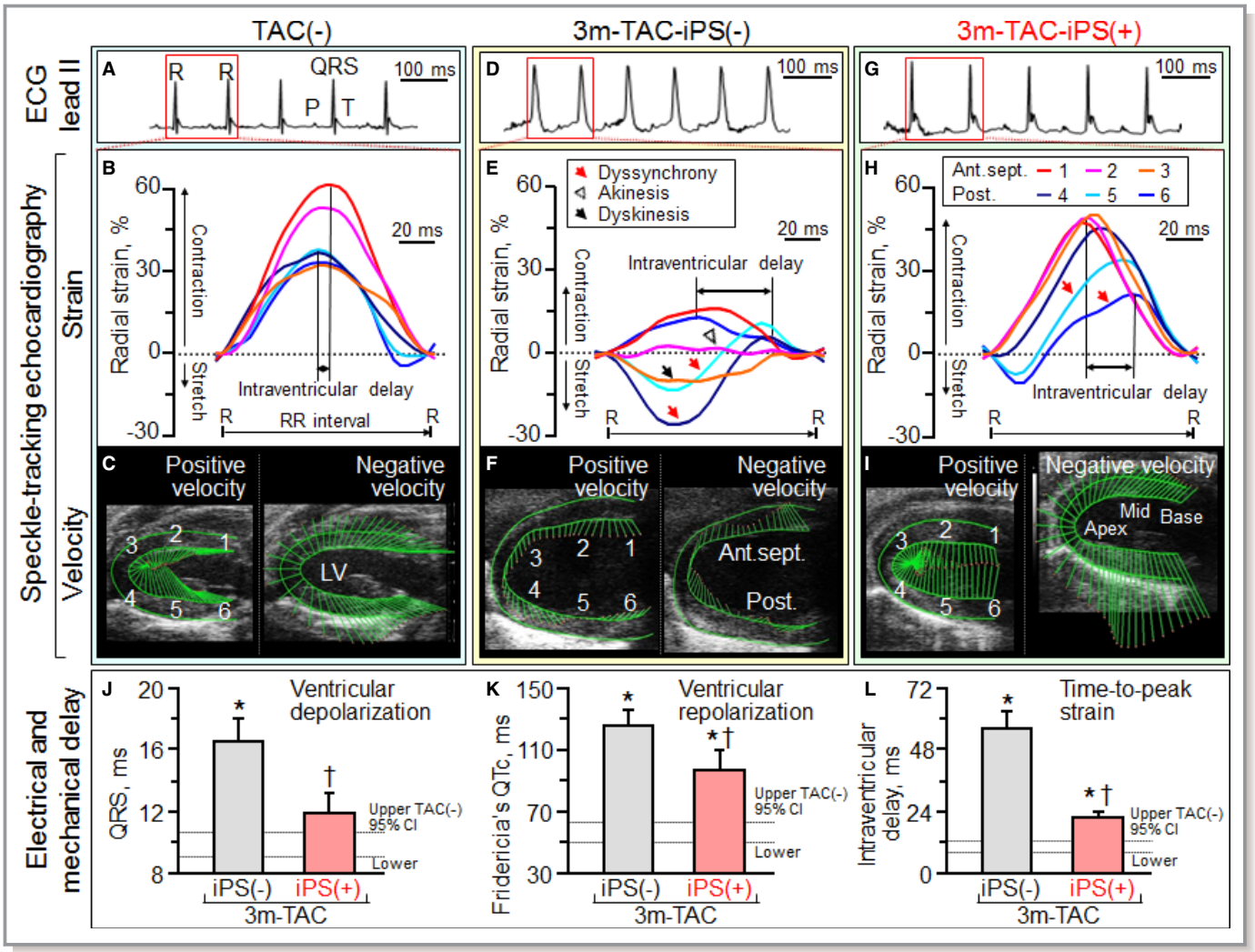

Figure 2. Stem cell intervention associated with synchronized ventricular conduction and contraction in *Kcnj11*-deficient stress-intolerant cardiomyopathy. ECG and speckle-tracking echocardiography in Kir6.2-deficient cohorts: without stress imposition [TAC(−), A through C]; at 3 months of TAC without [TAC-iPS(−), D through F] or with iPS cell implantation [TAC-iPS(+), G through I]. QRS widening (J), QT prolongation (K), and intraventricular delay in time-to-peak strain (L), that characterized TAC-iPS(−) hearts, were minimized by epicardial delivery of 200 000 stem cells/heart. **P*<0.05 vs. TAC(−); †*P*<0.05 vs. TAC-iPS(−). 1 indicates basal anterior-septum (Ant.sept.); 2, mid-Ant.sept.; 3, apical Ant.sept.; 4, apical posterior wall (Post.); 5, mid-Post.; 6, basal Post.; CI, confidence interval; Fridericia's QTc, QT interval corrected by Fridericia's formula; iPS, induced pluripotent stem; LV, left ventricle; R–R, R–R interval; TAC, transverse aortic constriction.

catheterization.[23] LV volumes, dimensions, wall thicknesses, and mass were measured/calculated from 2D or 2D-targeted M-mode echocardiography through the aligned parasternal long-axis acoustic window following guidelines of the American Society of Echocardiography.[24] Ejection fraction (%), fractional shortening (%), systolic-to-diastolic ratio of wall thickness (%), and average peak strain values were calculated as echocardiography-based parameters of LV contractility. Systolic and end-diastolic LV pressures were evaluated by a 1.4-F micropressure catheter (SPR-671; Millar Instruments, Houston, TX; MPVS-400; ADInstruments, Colorado Springs, CO), and first derivatives were extrapolated.

Dyssynchrony Monitoring

Heart rate and QRS/QT intervals were recorded by electrocardiography (LabChart 7; ADInstruments). QT intervals were corrected (QTc) for heart rate following the Fridericia's formula: $QTc=QT/(\text{R-R interval}/1000)^{1/3}$.[25] Speckle-tracking echocardiography (VevoStrain; FUJIFILM VisualSonics) was executed at a heart rate of 468±10 beats per minute (bpm) and frame rate of 240±12 frames per second. Animals surviving >2 months post-TAC displaying stable speckle-tracking tracing in all long-/short-axis segments, [7 TAC-iPS (−), 5 TAC-iPS(+)], were employed for speckle-based evaluation. Intraventricular mechanical discordance was calculated

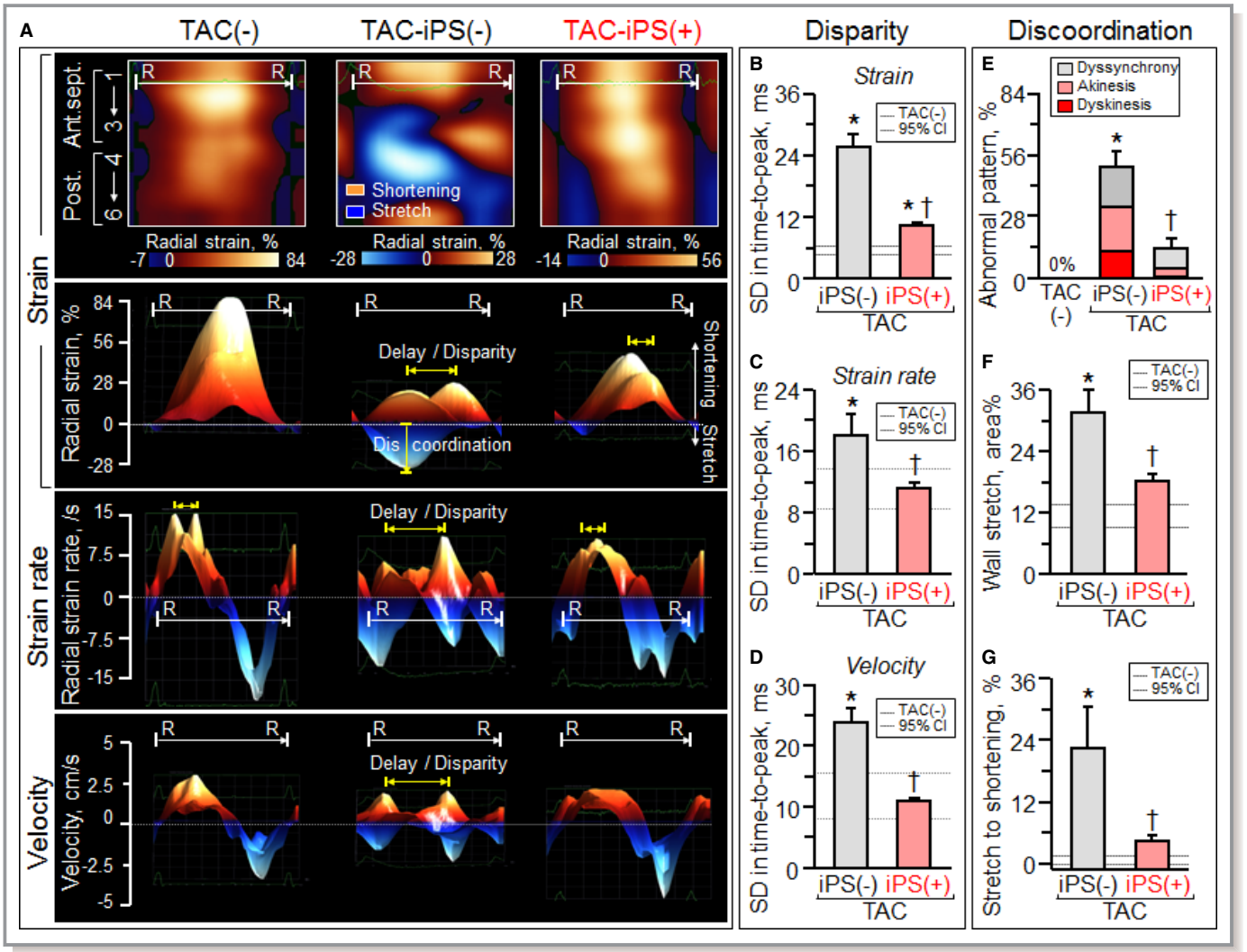

Figure 3. Impact of stem cell therapy on wall motion dynamics deconvoluted by speckle-tracking echocardiography. At 3 months poststress, untreated cardiomyopathic ventricles [TAC-iPS(−)] demonstrated decline in peak shortening, as well as disparity in timing and direction of tissue deformation (A). Cell intervention [TAC-iPS(+)] corrected delay/disparity in peak contraction (yellow arrows in A, B through D), discordant patterns (E), and conflicting tissue stretch (F and G), restoring patterns/values similar to prestress ventricles [TAC(−)]. *P<0.05 vs. TAC(−); †P<0.05 vs. TAC-iPS(−). 1 indicates basal anterior septum (Ant.sept.); 2, mid-Ant.sept.; 3, apical Ant.sept.; 4, apical posterior wall (Post.); 5, mid-Post.; 6, basal Post.; CI, confidence interval; iPS, induced pluripotent stem; R–R, R–R interval; SD, standard deviation; TAC, transverse aortic constriction.

as: (1) delay—difference in latest and earliest time-to-peak strain; (2) disparity—standard deviation of time-to-peak strain/strain rate/velocity; and (3) discoordination—area of myocardial stretch in strain/R-R interval map (%) and stretch-to-shortening ratio (%). Abnormal patterns were classified as dyssynchrony, akinesis, and dyskinesis.[22]

Heart Failure Syndrome

Systemic parameters, namely, arterial oxygen saturation (Mouse Ox; Starr Life Science, Oakmont, PA), maximum oxygen consumption (Oxymax; Columbus Instruments, Columbus, OH), exercise tolerance, and survivorship, were assessed. Treadmill (Columbus Instruments) protocols included endurance—a step-wise increase in incline and velocity at 3-minute intervals, and energy expenditure—at fixed speed of 10 m/minute and inclination of 20 degrees for 35 minutes.

Pathological Evaluation

Postmortem, heart and lung weights were measured and hematoxylin-eosin–stained heart, lung, liver, and spleen tissue were surveyed. Cardiac interstitial fibrosis was quantified by computerized imaging analysis (cellSens 1.3; Olympus, Tokyo,

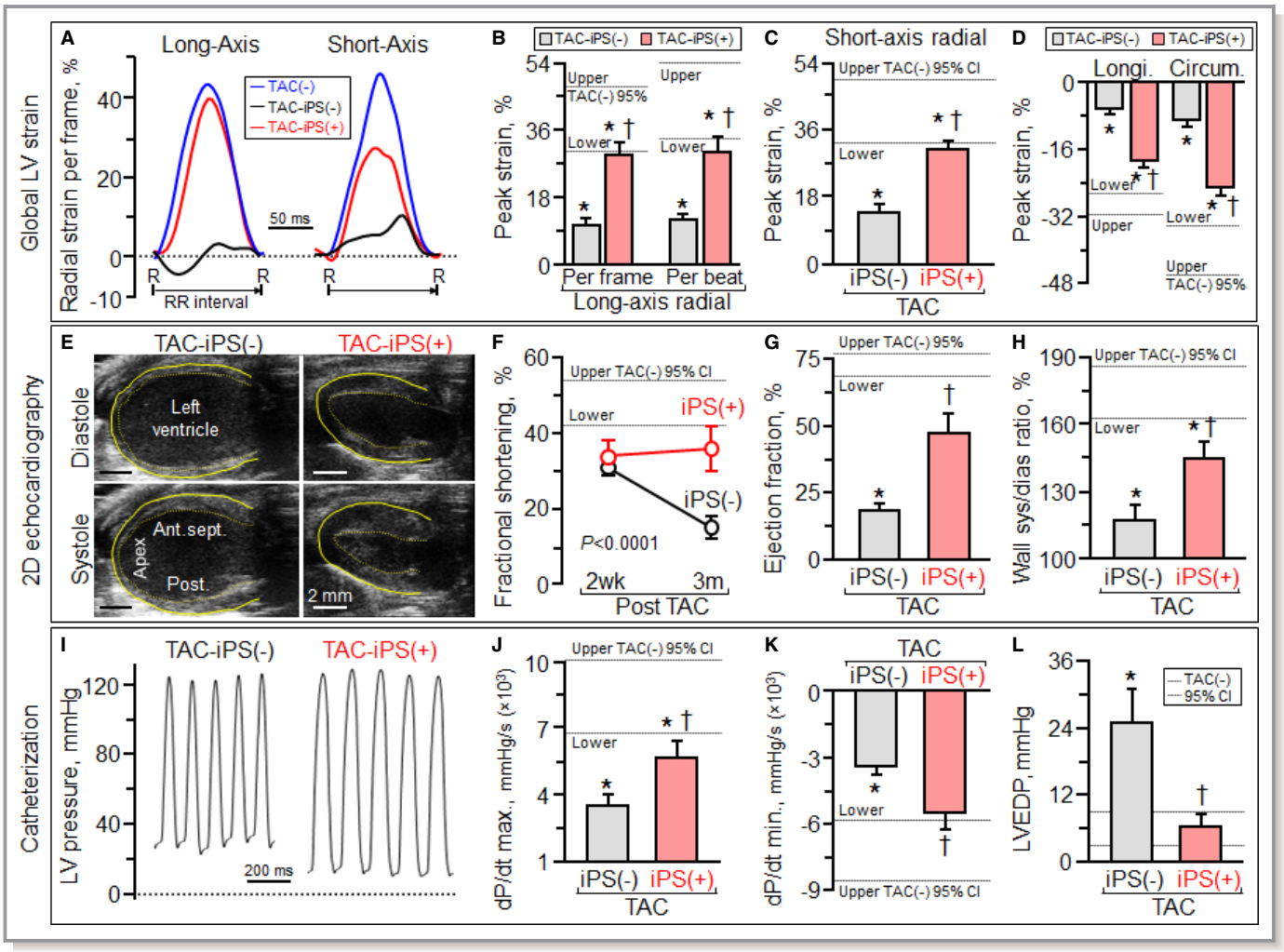

Figure 4. Benefit of stem cell intervention on cardiac performance and hemodynamics. At 3 months (3m) follow-up, iPS cell therapy, administered at 2 weeks post-TAC-iPS(+), rescued LV function, in contrast to unprotected TAC-stressed hearts not receiving cell therapy [TAC-iPS(−)]. Global and regional systolic function was superior in the TAC-iPS(+) group based on speckle strain (A through D), 2-dimensional (2D)/M-mode echocardiography (E through H), and catheterization (I and J) evaluation. Abnormal LV relaxation (K) and diastolic function (L), evident in untreated hearts, was prevented by stem cell therapy. *P<0.05 vs. TAC(−); †P<0.05 vs. TAC-iPS(−). Bar represents 2 mm in (E). Ant.sept. indicates anterior septum; CI, confidence interval; circum., circumferential; dP/dt max., maximum rate of change in LV pressure; dP/dt min., minimum rate of change in LV pressure; iPs, iPS, induced pluripotent stem; longi., longitudinal; LVEDP, left ventricular end-diastolic pressure; Post., posterior wall; R–R, R–R interval; TAC, transverse aortic constriction.

Japan) of phosphotungstic acid hematoxylin-stained sections. Myocardial disarray was evaluated by laser confocal microscopy (Zeiss LSM 510; Carl Zeiss, Thornwood, NY) following sarcomeric α-actinin (1:200; Sigma-Aldrich, St Louis, MO), along with nuclear 4′,6′-diamidino-2-phenylindole (Molecular Probes, Eugene, OR) staining. Cell proliferation and cardiac stem cells were evaluated by immunostaining for Ki67 (1:400; D3B5; Cell Signaling Technology, Danvers, MA) and Sca-1 (1:100; R&D Systems, Minneapolis, MN), respectively.[26] Engraftment of implanted iPS cells was tracked using a β-galactosidase antibody (1:5000; Abcam, Cambridge, MA). Ultrastructural evaluation, including percent area of myofibrils in cytoplasm,[27,28] was performed by transmission electron microscopy (JEOL 1200 EXII; JEOL Ltd, Tokyo, Japan).

Proteomics

LV protein extracts [10 Kir6.2-deficient LVs, 4 TAC(−), 3 TAC-iPS(−), 3 TAC-iPS(+)] were resolved by immobilized pH gradient 2D electrophoresis (pH 3 to 10) and silver stained. Differences across cohorts were identified using PDQuest gel image analysis (v.7.4.0; Bio-Rad, Hercules, CA), followed by mass spectrometry for protein assignment.[29] Reconstituted tryptic peptides were trap injected onto a ProteoPep C18 PicoFrit nanoflow column (New Objective, Woburn, MA) on an Eksigent nanoHPLC system (AB Sciex, Framingham, MA) coupled to an LTQ-Orbitrap (Thermo Fisher Scientific, Waltham, MA) mass spectrometer.[30] Mass spectra peptide identification was conducted with Mascot v.2.2 by screening

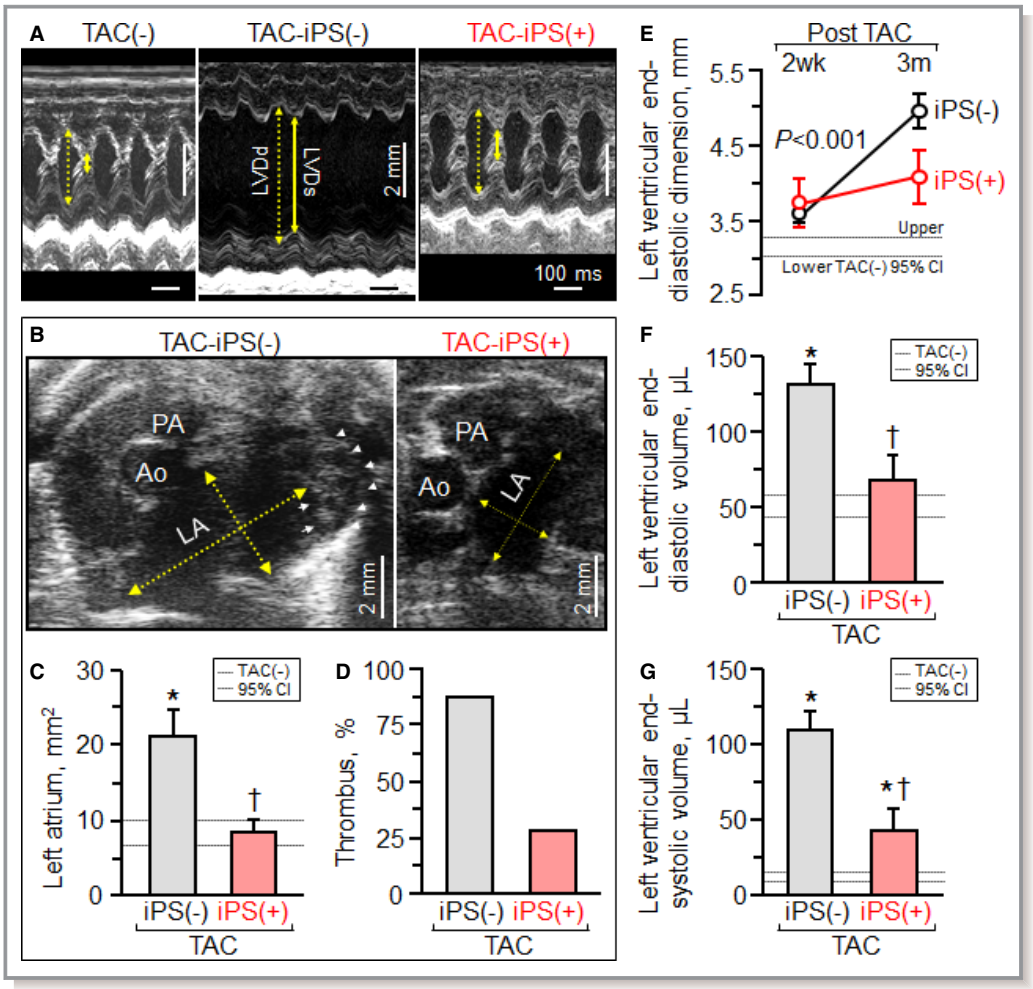

Figure 5. Reverse remodeling in stem cell-treated cardiomyopathy. Pressure overload imposed upon Kir6.2-deficient hearts [TAC-iPS(−)] induced pathological remodeling, which affected beyond the LV (A), the LA (B and C) with thrombosis (D), in line with LV systolic and diastolic failure. Stem cell therapy administered at an early stage of disease [TAC-iPS(+)] prevented increases in LV dimension (E) and volume (F and G). *P<0.05 vs. TAC(−); †P<0.05 vs. TAC-iPS(−). In (A) bar, 100 ms or 2 mm. In (B) yellow arrows, LA dimensions in short-axis view; arrow heads, thrombus in LA. Ao indicates aorta; CI, confidence interval; iPs, iPS, induced pluripotent stem; LA, left atrium; LV, left ventricle; LVDd (yellow dotted arrow in A), LV end-diastolic dimension; LVDs (yellow solid arrow in A), LV end-systolic dimension; PA, pulmonary artery; TAC, transverse aortic constriction.

sequences using Swiss-Prot (v.53.0; 53 539 entries). Searches tolerated 2 missed cleavages, ±0.01 Da error for precursor ions (including ^{13}C peak detection) and ±0.6 Da for product ions, allowing for protein N-terminal acetylation, methionine oxidation, and cysteine carbamidomethylation. Protein identities were confirmed by matching multiple peptide spectra at $P<0.05$, with proteins accepted at $P<0.01$. Differentially expressed proteins were submitted to Ingenuity Pathways Analysis (Ingenuity Systems, Redwood City, CA) for identification of overrepresented adverse cardiac outcomes.

Statistical Analysis

Analysis was performed in investigator-blinded fashion. Unless specified, numbers per group for noninvasive cardiac and systemic evaluation were WT animals: 8 in TAC(−) and 6 in TAC(+) at 2 weeks; *Kcnj11*-null mutants: 15 in TAC(−), 30 in TAC(+) at 2 weeks, and 21 in TAC(+) [14 TAC-iPS(−), 7 TAC-iPS(+)] at final follow-up. The nonparametric Mann-Whitney *U* test was used to evaluate significance (JMP 9; SAS Institute Inc., Cary, NC). The Student's *t*-test was employed to compare pre- and post-measurements in the same groups of animals. Comparison between groups over time was performed by 2-way repeated-measures ANOVA. Kaplan-Meier analysis with log-rank testing was applied for survival analysis. Proteomic comparison between groups was performed using a Student's *t*-test with data expressed as fold change. Cardiac adverse outcome overrepresentation was assessed using Fisher's exact test. Data are presented as mean±SEM. A *P* value <0.05 was predetermined as significant.

Results

Mechanical Discordance Responsive to Stem Cell Intervention

Under stress imposed by persistent TAC, adult *Kcnj11*-null mutants—but not WT counterparts—developed mechanical dyssynchrony-prone dilated cardiomyopathy (Figure 1). Within 2 weeks post-TAC, *Kcnj11*-null cardiomyopathic hearts had reduced LV ejection fraction (Figure 1A) with a narrow QRS-complex (Figure 1G and 1H). Nascent intraventricular mechanical discordance, defined by increased delay in peak contractions (Figure 1B through 1F), progressed

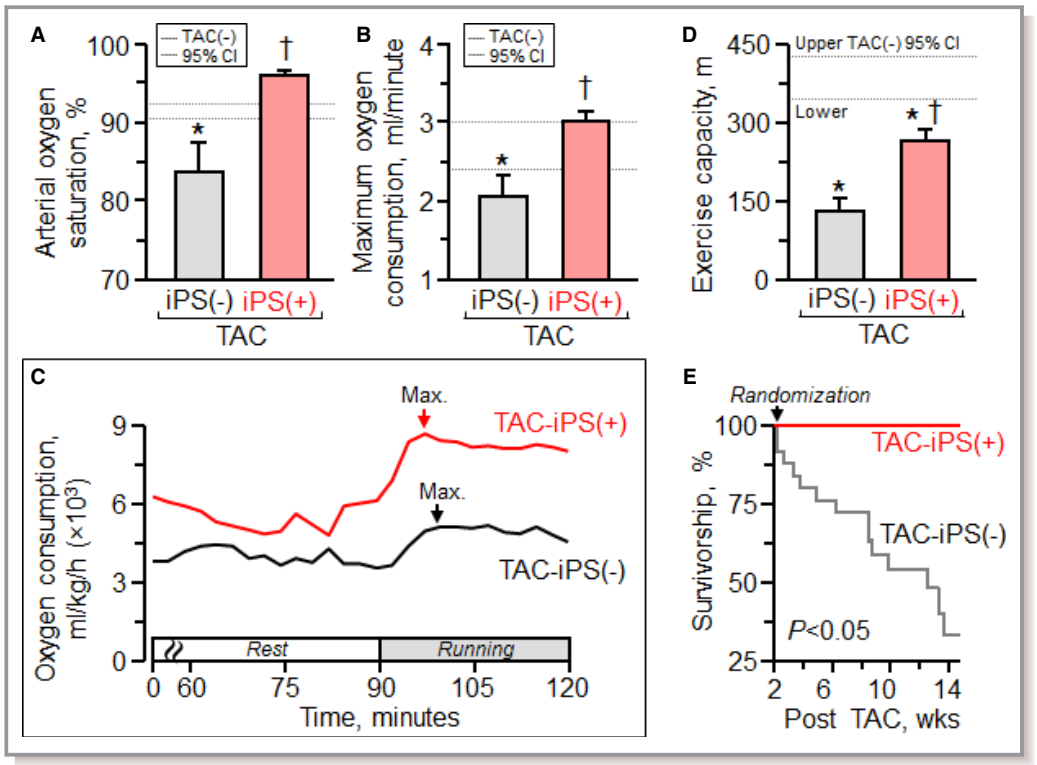

Figure 6. Rescue of the heart failure syndrome. In contrast to end-stage systemic heart failure prominent in untreated cardiomyopathy [TAC-iPS(−)], in the stem cell-treated cohort [TAC-iPS(+)], cardiac synchronization with reverse remodeling translated into maintained cardiopulmonary function (A), maximum oxygen consumption (B and C), and exercise capacity (D), with survival benefit (E). **P*<0.05 vs. TAC(−); †*P*<0.05 vs. TAC-iPS(−). CI indicates confidence interval; iPS, induced pluripotent stem; Max. (arrow in C), maximum oxygen consumption; TAC, transverse aortic constriction.

within 3 months of TAC-imposed stress into florid electromechanical dysfunction (Figure 2A through 2F). Epicardial delivery of 200 000 iPS cells/heart at 2 weeks post-TAC synchronized *Kcnj11*-deficient cardiomyopathic hearts (Figure 2G through 2I). Transplant of iPS cells minimized prolongation of the QRS-complex and QTc interval without a change in heart rate, otherwise prominent at 3 months [QRS, 10.1±0.4 ms in prestress, 16.5±1.5 ms in TAC-iPS(−), 11.9±1.3 ms in TAC-iPS(+), $P<0.05$, TAC-iPS(−) versus TAC-iPS(+), Figure 2J; QTc, 56.8±2.9 ms in prestress, 125.5±10.1 ms in TAC-iPS(−), 96.7±12.6 ms in TAC-iPS(+), $P<0.05$, TAC-iPS(−) versus TAC-iPS(+), Figure 2K; heart rate, 489±14 bpm in prestress, 466±23 bpm in TAC-iPS(−), 486±27 bpm in TAC-iPS(+), $P=0.54$, TAC-iPS(−) versus TAC-iPS(+)]. Stem cell therapy shortened intraventricular delay in time-to-peak strain, reflecting correction of discordant wall motion [56.1±6.6; wks, weeks ms in TAC-iPS(−) versus 21.5±2.5 ms in TAC-iPS(+), $P<0.01$, Figure 2L]. The impact of stem cell intervention on wall motion dynamics was deconvoluted in R-R interval/anatomical maps (Figure 3A top), as well as in R-R interval/strain, strain rate, or velocity maps (Figure 3A). iPS cell delivery lessened the TAC-reduced peak shortening and alleviated conflicting wall motions in systole/diastole (Figure 3A). Cell transplantation maintained a normokinetic biphasic pattern, eliminating distorted patterns observed in untreated hearts (Figure 3A). Benefit of the stem cell intervention was consistent across long- and short-axis radial, longitudinal, and circumferential components. Standard deviation of time-to-peak in deformation imaging (ie, disparity in timing

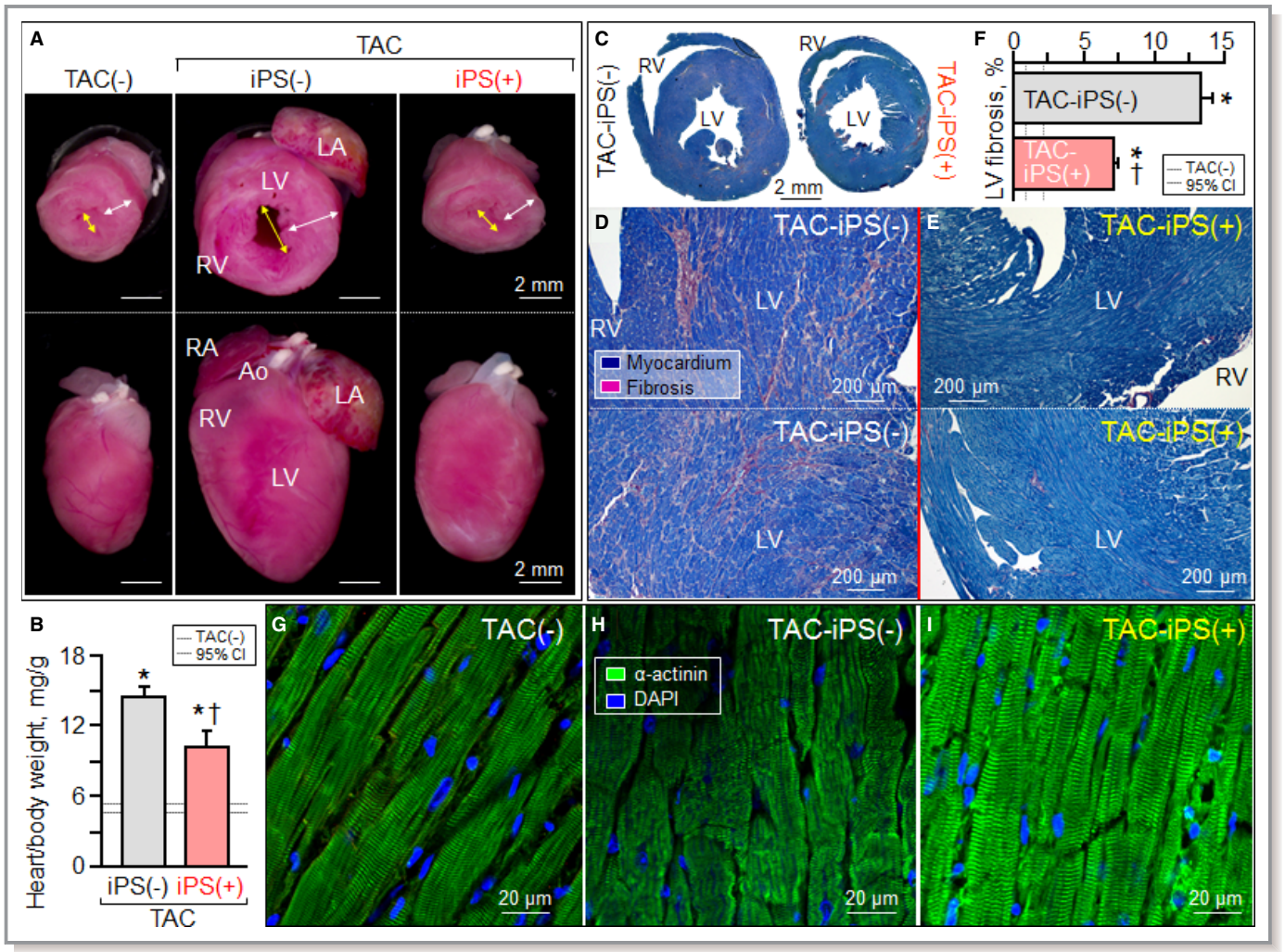

Figure 7. Protection of organ geometry and histology. Exaggerated cardiomegaly (A and B), fibrosis (C through F), and myocardial disarray (G through I) in response to [TAC-iPS(-)] was blunted by stem cell therapy [TAC-iPS(+)]. *$P<0.05$ vs. TAC(−); †$P<0.05$ vs. TAC-iPS(−). Bar represents 2 mm in (A). Ao indicates aorta; CI, confidence interval; DAPI, 4′,6′-diamidino-2-phenylindole; iPS, induced pluripotent stem; LA, left atrium; LV, left ventricle; RA, right atrium; RV, right ventricle; TAC, transverse aortic constriction; white arrow, LV free wall; yellow arrow, LV dimension; α-actinin, sarcomeric α-actinin.

of tissue contraction) was stabilized by Stem cell therapy (strain, $P<0.0001$, Figure 3B; strain rate, $P<0.05$, Figure 3C; velocity, $P<0.001$, Figure 3D). Parameters of discoordination, namely, abnormal patterns ($P<0.001$, Figure 3E), stretch ($P<0.01$, Figure 3F), and stretch-to-shortening ratio ($P<0.05$, Figure 3G), were corrected in stem cell-treated hearts. Thus, iPS cell intervention into a mechanically dyssynchronous heart aborted worsening in discordant wall motion.

Synchronization Protects Cardiac Function and Structure

At 3 months post-TAC, iPS cell-treated *Kcnj11*-null hearts remained synchronous (Figure 3) and exhibited proper systolic contraction and diastolic relaxation (Figure 4A). In contrast, in untreated dilated cardiomyopathic hearts, abnormal systolic stretch followed by delayed contraction underlined poor pump function (Figure 4A through 4D). Serial echocardiography demonstrated severe LV hypokinesis (Figure 4E through 4H) and dilatation with wall thinning in the sham group (Figure 4E left), whereas LV wall motion and thickness were preserved in iPS cell-treated hearts (Figure 4E right). Fractional shortening decreased in sham hearts from 31.2±3.1% at 2 weeks post-TAC to 15.3±2.9% at 3 months post-TAC ($P<0.0001$), yet was maintained in iPS cell-treated hearts from 34.0±3.9% to 35.9±6.0% over the same period [TAC-iPS(−) versus TAC-iPS(+) at 3 months post-TAC, $P<0.0001$, Figure 4F]. Notably, ejection fraction was higher in the iPS cell-treated cohort [TAC-iPS(−) 18.1±2.8%, TAC-iPS (+) 47.4±7.2%, $P<0.001$, Figure 4G]. Overall, iPS cell-treated cardiomyopathic hearts displayed improved hemodynamics

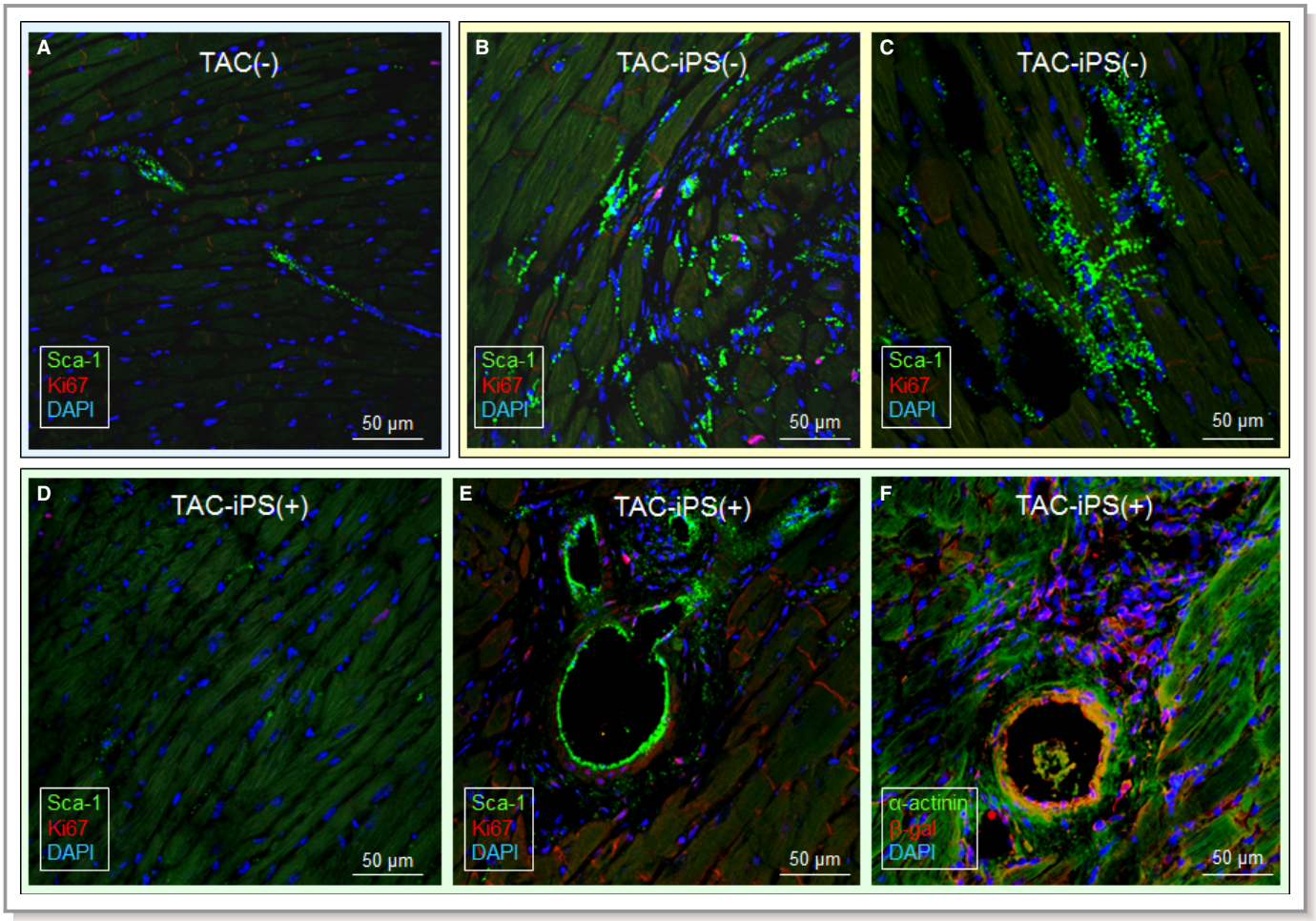

Figure 8. Long-term, limited engraftment of implanted stem cells. Chronic (3 months) stress, imposed by TAC upon Kir6.2-deficient hearts, mobilized endogenous Sca-1$^+$ stem cells from the perivascular niche prestress [TAC(−); A] to the myocardial parenchyma [TAC-iPS(−); B and C]. In stem cell-treated ventricles under equivalent TAC-induced stress [TAC-iPS(+)], Sca-1$^+$ cells were recruited into the perivascular stem cell niche and colocalized with transplanted stem cells tracked by β-galactosidase expression (D through F). CI indicates confidence interval; DAPI, 4′,6′-diamidino-2-phenylindole; iPS, induced pluripotent stem; TAC, transverse aortic constriction; α-actinin, sarcomeric α-actinin; β-gal, β-galactosidase.

(Figure 4I through 4L) with normalized LV end-diastolic pressure [TAC-iPS(−) 24.8±6.2 mm Hg, n=5, TAC-iPS(+) 6.4±2.1 mm Hg, n=6, $P<0.01$, Figure 4I and 4L]. Functional benefit was associated with halted structural maladaption (Figure 5), and protection against LV dilatation (Figure 5A), atrial enlargement and thrombosis (Figure 5B through 5D). LV diastolic dimension increased from 3.60±0.13 mm at 2 weeks post-TAC to 4.94±0.22 mm at 3 months post-TAC without cell therapy, whereas iPS cell-treated hearts demonstrated stable dimensions maintained from 3.73±0.32 to 4.07±0.36 mm [$P=0.46$, TAC-iPS(−) versus TAC-iPS(+) at 2 weeks post-TAC; $P<0.001$, TAC-iPS(−) versus TAC-iPS(+) at 3 months; Figure 5E]. Expansion in LV diastolic/systolic volume was diminished by iPS cell therapy (Figure 5F and 5G). Thus, mechanical and electrical synchronization observed in the iPS cell-treated cohort was associated with protected cardiac performance and reverse remodeling.

Rescue of Heart Failure Syndrome

The benefit of iPS cell intervention translated prospectively into mitigation of HF syndrome. iPS cell treatment reduced lung congestion [lung weight, 172.2±7.5 mg in prestress, 418.1±39.9 mg in TAC-iPS(−), 291.6±41.9 mg in TAC-iPS(+), $P<0.05$, TAC-iPS(−) versus TAC-iPS(+)] and preserved arterial oxygen saturation ($P<0.01$, Figure 6A), maximal oxygen consumption ($P<0.01$, Figure 6B and 6C), and aerobic exercise capacity ($P<0.0001$, Figure 6D). Mortality was not observed in the iPS cell-treated cohort, in contrast to high mortality rates observed without iPS cell intervention [survivorship 3 months postrandomization, 33.9% in TAC-iPS(−),100% in TAC-iPS(+), $P<0.05$, Figure 6E]. Of note, there was no sign of uncontrolled growth upon macroscopic and microscopic evaluations of heart, lung, liver, and spleen in iPS cell-treated animals, indicating long-term tumor-free survivorship. Thus, iPS cell therapy of dyssynchrony-prone cardiomyopathy precluded progression of HF syndrome.

Cell Therapy Corrects Cardiomyopathic Substrate

Cardiomegaly and pathological increase in organ weight were blunted by iPS cell therapy (Figure 7A and 7B). LV mass-to-body weight ratio was exaggerated in the sham group [4.18±0.32 mg/g in prestress, 9.25±1.10 mg/g in sham-treated TAC-iPS(−)]. In the absence of stem cell treatment, cardiomyopathic ventricles exhibited severe fibrosis [13.3±0.8% in TAC-iPS(−), n=45 sections, Figure 7C through 7F] and myofibrillar disarray (Figure 7G and 7H). In contrast,

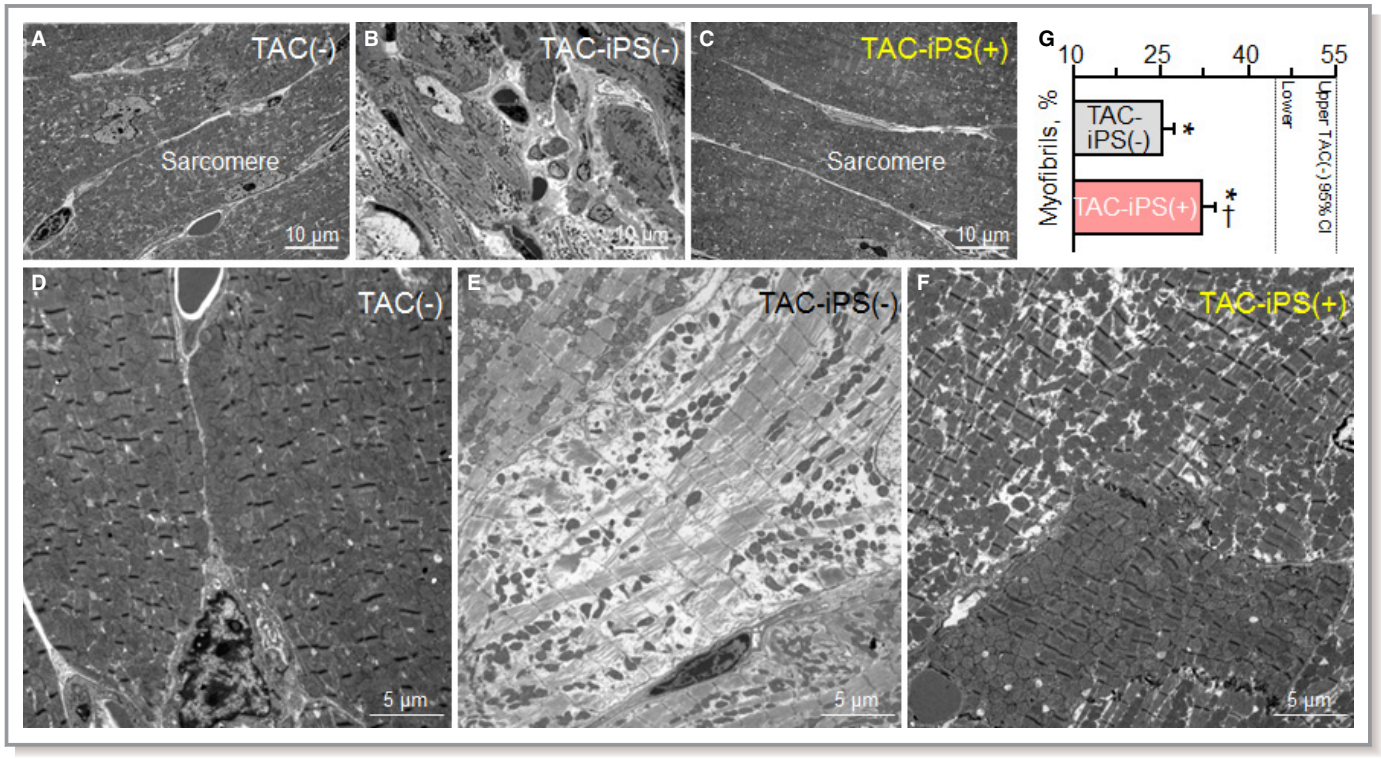

Figure 9. Protection of myofibrillar ultrastructure. Sarcomere ultrastructure at low- (A through C) and high-magnification (D through F) electron microscopy. Kir6.2-deficient left ventricles after 3 months of TAC demonstrated severe fibrosis [TAC-iPS(−); B] and lacked myofibrils (E). Cell-treated Kir6.2-deficient ventricles [TAC-iPS(+)] exhibited normal sarcomeres (C) with significant increase in myofibrils (F and G). *$P<0.05$ vs. TAC(−); †$P<0.05$ vs. TAC-iPS(−). CI indicates confidence interval; iPS, induced pluripotent stem; TAC, transverse aortic constriction.

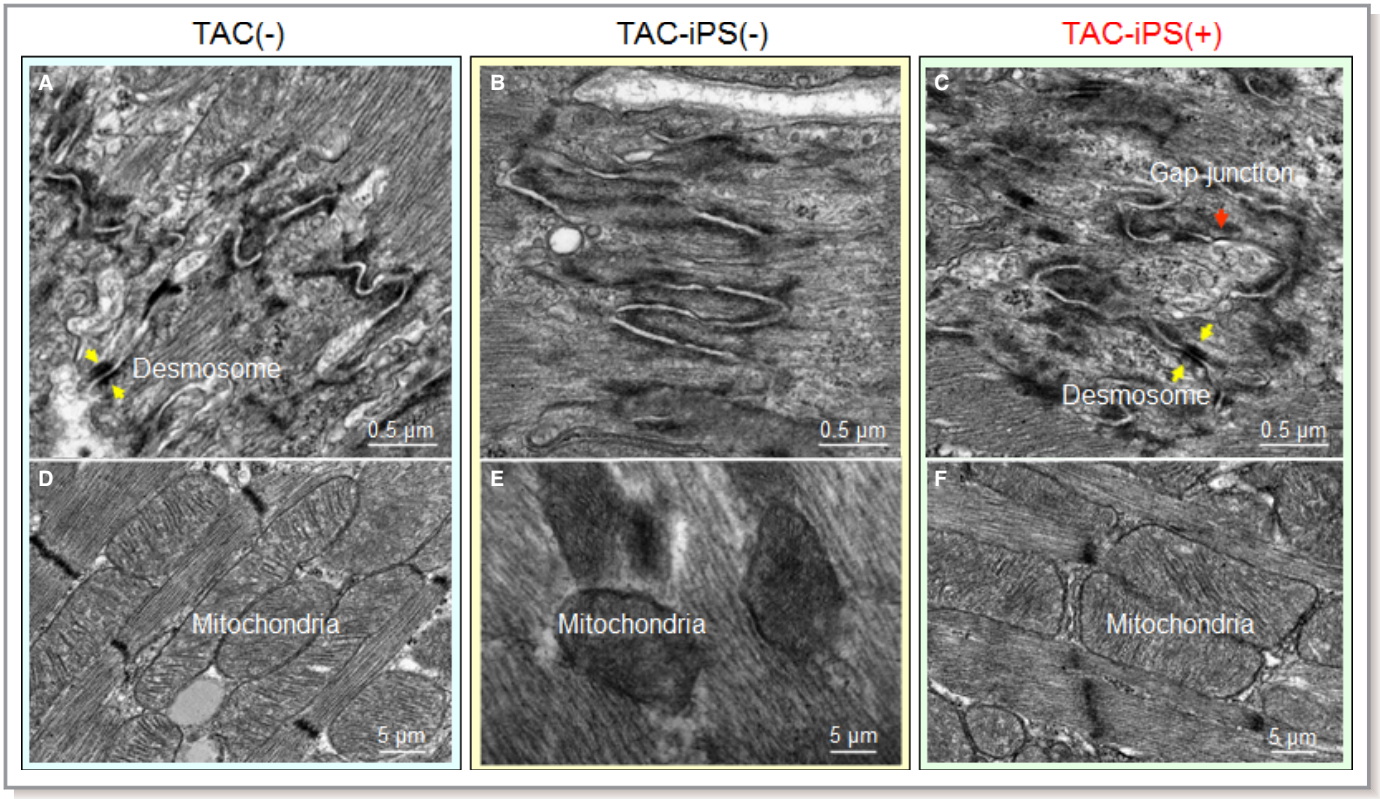

Figure 10. Protection of mitochondria and gap junction. Desmosomal (A through C) and mitochondrial (D through F) ultrastructure of Kir6.2-deficient left ventricles in 3 conditions: without stress imposition [TAC(−)]; TAC without therapy [TAC-iPS(−)]; or with stem cell therapy [TAC-iPS (+)]. Absence of clear gap junction formation (B) and disorganized, low-density mitochondria (E) observed in untreated ventricles was corrected by cell therapy (C and F). iPS indicates induced pluripotent stem; TAC, transverse aortic constriction.

iPS cell-treated cardiomyopathic hearts displayed limited fibrosis [7.0±0.4% in TAC-iPS(+), n=82 sections, $P<0.0001$ versus TAC-iPS(−); Figure 7C, 7E, and 7F] and maintained organized sarcomeres (Figure 7I). Stem cells demonstrated a distinct distribution pattern in iPS cell-treated versus untreated cardiomyopathic cohorts (Figure 8). Prestress ventricles exhibited a limited number of Sca-1^+ endogenous stem cells within the perivascular stem cell niche (Figure 8A). Poststress, fibrotic ventricles in the absence of iPS cell therapy displayed a deregulated Sca-1^+ cell mobilization pattern within the myocardial parenchyma [Sca-1^+ cells in parenchyma, 0.7±0.5% in prestress, n=7 sections, 10.7±2.4% in TAC-iPS (−), n=7 sections, $P<0.001$, Figure 8A through 8C]. In contrast, post-iPS cell therapy, endogenous Sca-1^+ cells adopted a normal distribution pattern away from myocardial parenchyma, in favor of the perivascular stem cell niche [Sca-1^+ cells in parenchyma, 1.3±0.8% in TAC-iPS(+), n=6 sections, $P<0.001$ versus TAC-iPS(−), Figure 8D through 8F]. Cell-based impact was further verified at the ultrastructural level (Figure 9). Whereas untreated cardiomyopathy was characterized by lack of contractile elements [percent area of myofibrils in cytoplasm, 49.6±2.5% in prestress, n=20 sections, 25.1±2.0% in TAC-iPS(−), n=20 sections, $P<0.0001$; Figure 9D, 9E and 9G], myofibrillar structures were significantly increased by stem cell therapy [32.1±2.3% in TAC-iPS(+), n=20 sections, $P<0.05$ versus TAC-iPS(−); Figure 9F and 9G]. In addition to antifibrotic and promyogenic effects, cell therapy protected gap junction and desmosome structures (Figure 10A through 10C) and sustained mitochondria density (Figure 10D through 10F). Beyond histological assessment, molecular outcomes were profiled by high-throughput proteomics (Figure 11A). Mass spectrometric analysis and peptide assignment (eg, Figure 11B, 11C, and Table S1) delineated 205 down-regulated and 52 up-regulated proteins arising from the response to cell therapy (Table S2). Stem cell therapy abolished 48 TAC-induced protein changes (Figure 12A) accounting for 44% of the cardiomyopathic proteome (Figure 12B). Moreover, stem cell intervention nullified 86% of TAC-induced alterations in proteins with canonical links to cardiac disease [asterisk (*) in Figure 12A and 12C], demonstrating nonstochastic overhaul of the cardiomyopathic proteome. Overrepresented adverse cardiac outcomes, predicted to be associated with dyssynchronous cardiomyopathy on the basis of proteomic findings, were counteracted by cell therapy (Figure 12D). Thus, iPS cell therapy appears to correct the disease substrate underlying dyssynchronous cardiomyopathy.

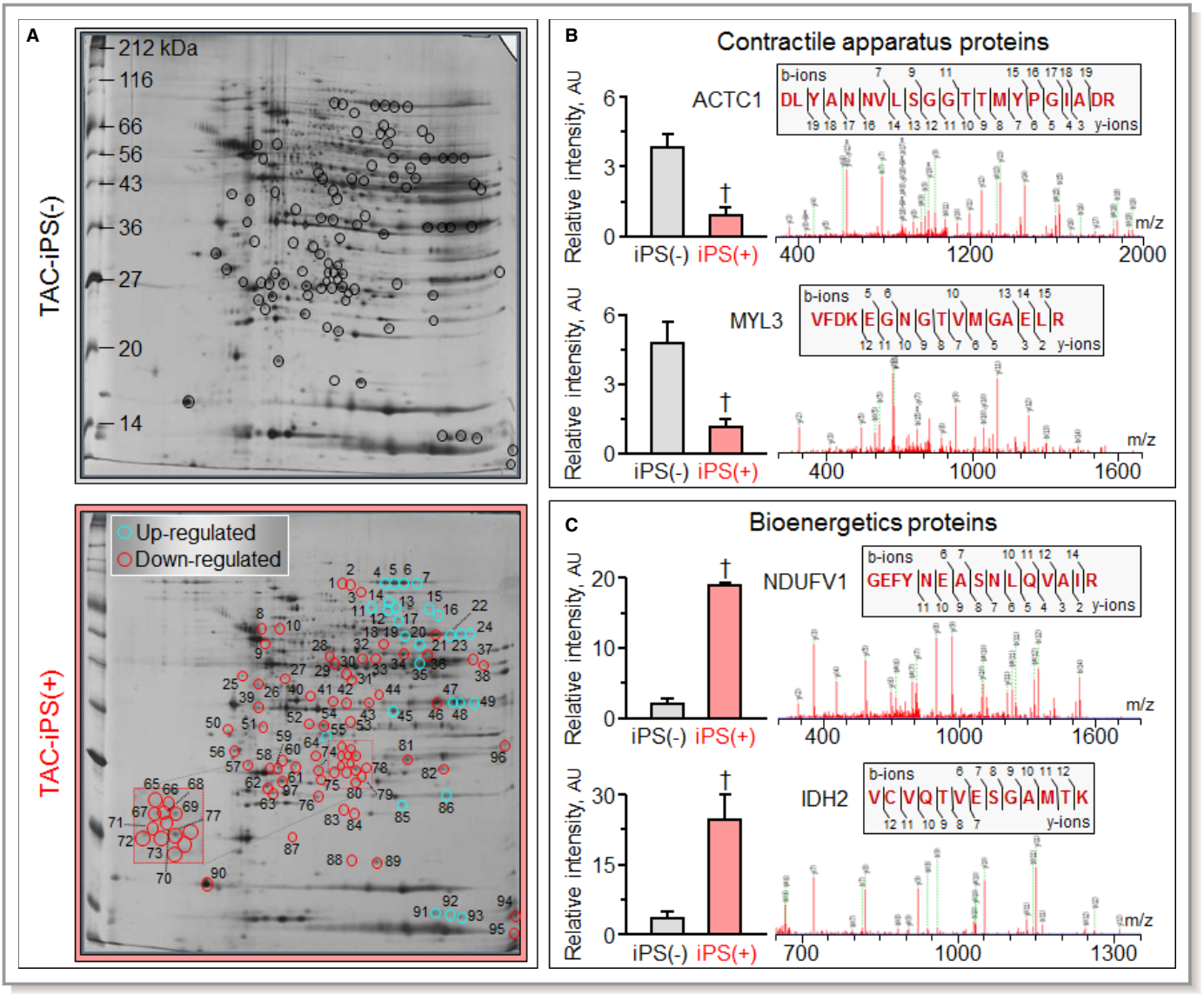

Figure 11. Peptide identification and assignment of representative proteins down- or up-regulated by stem cell therapy. Representative 2-dimensional gels of left ventricular cytoplasmic protein extracts (100 μg per gel) from stress-induced cardiomyopathy without [TAC-iPS(−)] and with iPS cell therapy [TAC-iPS(+)] resolved by pH 3 to 10 IEF, 12.5% SDS-PAGE (A). Statistical analysis after gel densitometric spot quantitation revealed 97 differentially expressed (fold change >1.5, $P<0.05$) protein spots, circled and numbered, from which mass spectrometric analysis assigned identities to down- and up-regulated proteins. LTQ-Orbitrap MS/MS product ion spectra obtained are shown for representative contractile apparatus proteins down-regulated in response to cell therapy (B), including ACTC1 (spot 28) and MYL3 (spot 58), and bioenergetics proteins up-regulated by cell therapy (C), including NDUFV1 (spot 22) and IDH2 (spot 23). Histographs indicate relative spot intensities without [iPS(−)] or with cell treatment [iPS(+)], whereas Mascot spectra indicate detected b- and y-ions, with corresponding peptide sequence identified and assigned to the protein (upper insets). ACTC1 indicates alpha cardiac actin; AU, arbitrary units; IDH2, isocitrate dehydrogenase 2 [NADP], mitochondrial; IEF, isoelectric focusing; iPS, induced pluripotent stem; MS/MS, tandem mass spectrometry; m/z, mass-to-charge ratio of detected ion species; MYL3, myosin light chain 3; NDUFV1, NADH dehydrogenase flavoprotein subunit 1; TAC, transverse aortic constriction.

Discussion

The present study assessed the potential of a stem cell-based intervention on narrow QRS-complex HF. Using a model of adult-onset dilated cardiomyopathy, we report that myocardial administration of iPS cells, early in disease, synchronized wall motion and precluded organ decompensation. Functional benefit was supported by reverse remodeling and normative restitution of the disease proteome. Stem cell biotherapy thus potentially shows promise as a means to protect pump function in the setting of mechanical dyssynchrony-prone HF.

Success afforded by device-based CRT points to cardiac dyssynchrony as a legitimate target for intervention in HF.[31,32]

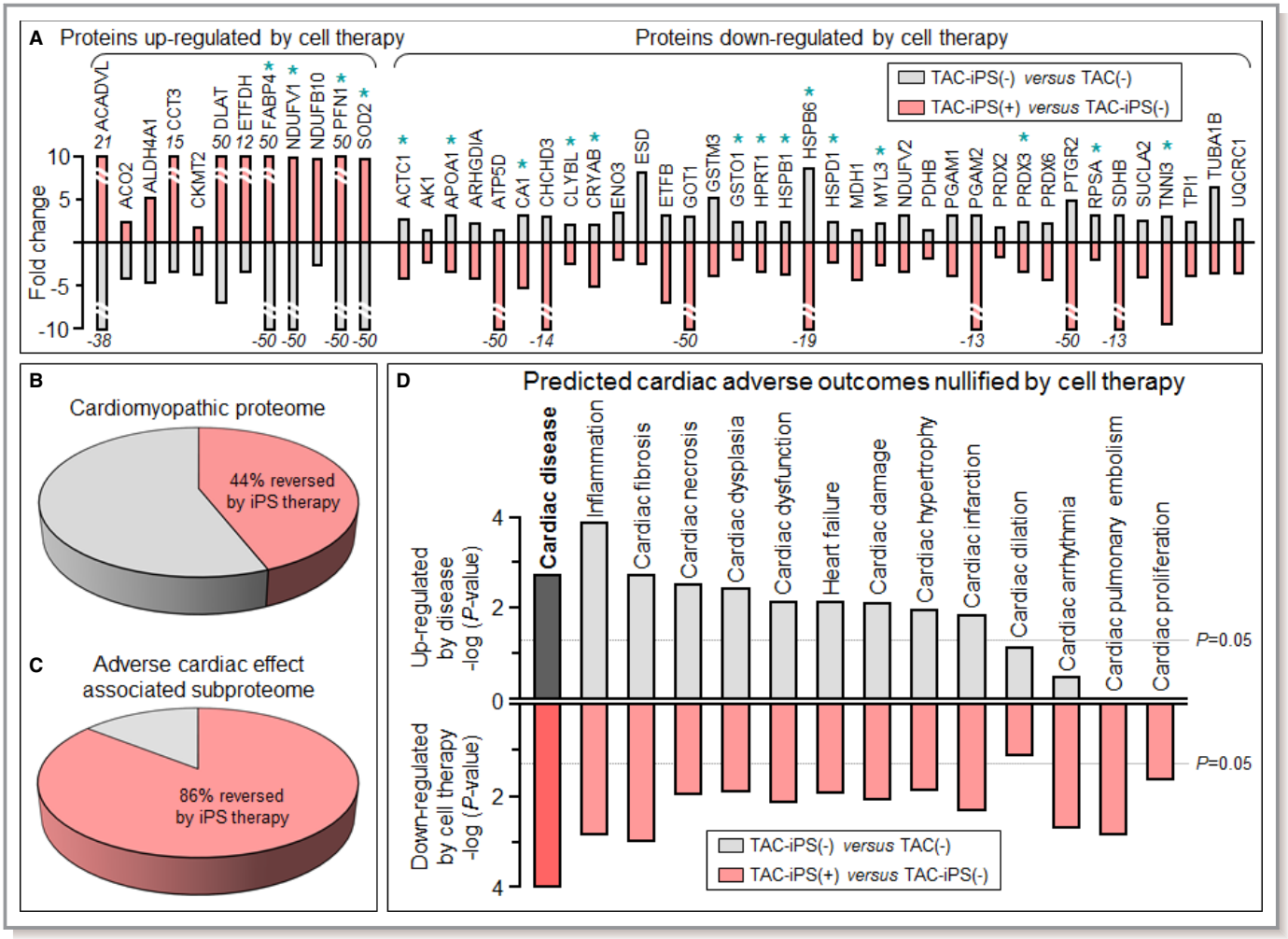

Figure 12. Cardiomyopathic proteome restitution. A subset of 48 proteins was reversed by iPS cell therapy, significantly altered [red, TAC-iPS (+)] in the opposite direction to their initial significant change in response to disease [gray, TAC-iPS(−)], including 18 proteins (*) with established links to cardiac adverse effects (A). The 48 reversed proteins account for 44% (48 of 109) of resolved cardiomyopathic proteome changes (B) and 86% (18 of 21) of cardiomyopathic protein changes having canonical links to adverse cardiac outcomes (C). In response, all adverse cardiac outcomes predicted by hypergeometric overrepresentation analysis of the initial cardiomyopathic proteome (gray) were nullified by cell therapy (red; D). iPS indicates induced pluripotent stem; TAC, transverse aortic constriction.

However, the reach of bi-ventricular pacing across a diverse spectrum of dyssynchronous HF substrates remains uncertain.[33] A case in point is mechanical dyssynchrony developing in the absence of QRS widening, which recent clinical trials pinpoint as unresponsive to CRT in the absence of conduction block.[34–38] As CRT necessitates a responsive contractile myocardium, which is compromised in primary myocardial disease,[39,40] the present study explored a reparative approach aimed at correcting the dyssynchronous substrate, at least in this small animal model.

Conventional dyssynchrony models recapitulate mechanical malfunction occurring simultaneously or following an electrical defect.[41,42] Herein, the dilated cardiomyopathy model generated mechanical dyssynchrony prior to electrical or systemic disease, providing a unique opportunity to longitudinally evaluate responsiveness to intervention. Monitoring progressive dyssynchrony in a non-left-bundle-branch-block setting was made possible through high-resolution imaging applicable to transgenic HF models.[22] Leveraging the nuclear reprograming technology, derived iPS cells were utilized due to a capacity to rebuild functional heart tissue, in ischemic heart disease.[43–45] Transplanted into infarcted myocardium, iPS cells achieve multilineage reconstruction.[20,46,47] iPS cell delivery, here, into dilated cardiomyopathic tissue prevented progression of dyssynchronous HF, possibly expanding indications to nonischemic heart disease.

Specifically, the present study documents, in the iPS cell-treated cohort, restoration of cardiac mechanics, recognized as an integral readout for cardiac repair.[48] The implemented stem cell intervention demonstrated effectiveness across

hierarchical endpoints, addressed at molecular, cellular, regional, and global levels, that collectively ensure adequate heart pump function.[49] Phenotype rescue was supported by a renovated proteome. Indeed, proteomic deconvolution unmasked a complex signature underlying the pathobiology of mechanical dyssynchrony-prone HF, with expression of 86% of all cardiac disease proteins apparently corrected by stem cell therapy. Ultrastructural assessment identified protection of the sarcomere, mitochondria, and cell-to-cell organization. Moreover, successful synchronization correlated with a favorable impact on sarcomeres and mitochondria, consistent with outcomes observed with device-based CRT.[50] Salvage of the disease substrate translated in vivo into improved wall motion dynamics documented by tissue deformation imaging, a sensitive noninvasive readout of myocardial dysfunction.[51–53] Synchronized ventricular motion invigorated pump function, with prevention of late-onset electrical abnormalities, and stabilization of organ geometry, leading to systemic and survival benefit. The value of cell-based synchronization was thus documented across vital symptomatology, as well as clinically relevant endpoints. The present study timed the early intervention based on wall motion abnormality, and displayed more-prominent benefit on contractile parameters, than on structural parameters, highlighting the prospect of substrate-specific markers for disease management.[54] The complexity in the regulation of cardiac mechanics, and the study design focused on prospective in vivo imaging, prevented delineation of the relationship of stem cell injection on mechanical dyssynchrony and myocardial contractility. Restoration of endogenous Sca-1$^+$ cells within the perivascular stem cell niche is consistent with recent reports recognizing niche-regulated processes, including a potentially significant contribution of paracrine mechanisms, protecting against fibrosis and decompensation after injury.[55,56] Dysregulation of Sca-1$^+$ distribution away from the perivascular niche suggests a maladaptive response to stress, which is corrected through stem cell intervention.[57] Whereas this study used *Kcnj11*-null mutants, iPS cell therapy has been documented as beneficial in dyssynchronous WT animals postinfarction,[41] indicating that efficacy of iPS cells is not limited to Kir6.2 deficiency. Mouse models expand the scope of cardiac dyssynchrony research, inviting further studies to recapitulate clinical features across the disease spectrum.[58,59]

In conclusion, a biological approach to address mechanical dyssynchrony in narrow QRS-complex cardiomyopathy was tested here. iPS cell-based intervention demonstrated signs of efficacy in restoring cardiac mechanics at functional and structural levels, translating into global rescue of HF syndrome. This proof-of-concept study provides initial, preclinical evidence of cell-based synchronization in the setting of dyssynchronous narrow QRS HF, introducing device-independent resynchronization in dilated cardiomyopathy.

Sources of Funding

This work was supported by the National Institutes of Health (R01HL64822, T32HL07111), American Heart Association, Leducq Fondation, Marriott Heart Disease Research Program, and Mayo Clinic Center for Regenerative Medicine. Dr Terzic holds the Marriott Family Professorship in Cardiovascular Research and is the Michael S. and Mary Sue Shannon Director, Mayo Clinic Center for Regenerative Medicine.

Acknowledgments

The authors thank Jonathan J. Nesbitt, Lois A. Rowe, Diane M. Jech, Courtney Rust, Nicolas L. Carlblom, Sarah Burrington, Andrea Clement, Maxwell J. Klepper, and Brock K. Johnson for assistance, as well as the Mayo Clinic Proteomics Research Center and NMR Core Facility for guidance in data acquisition. The authors are grateful to Drs Takashi Miki (Chiba University, Chiba, Japan) and Susumu Seino (Kobe University, Kobe, Japan) for initial derivation of the knockout model.

Disclosures

None.

References

1. 2013 ACCF/AHA guideline for the management of heart failure: a report of the American College of Cardiology Foundation/American Heart Association Task Force on Practice Guidelines. *J Am Coll Cardiol*. 2013;62:e147–e239.
2. Goldenberg I, Kutyifa V, Klein HU, Cannom DS, Brown MW, Dan A, Daubert JP, Estes NA III, Foster E, Greenberg H, Kautzner J, Klempfner R, Kuniss M, Merkely B, Pfeffer MA, Quesada A, Viskin S, McNitt S, Polonsky B, Ghanem A, Solomon SD, Wilber D, Zareba W, Moss AJ. Survival with cardiac-resynchronization therapy in mild heart failure. *N Engl J Med*. 2014;370:1694–1701.
3. Leyva F, Nisam S, Auricchio A. 20 years of cardiac resynchronization therapy. *J Am Coll Cardiol*. 2014;64:1047–1058.
4. Ruschitzka F, Abraham WT, Singh JP, Bax JJ, Borer JS, Brugada J, Dickstein K, Ford I, Gorcsan J III, Gras D, Krum H, Sogaard P, Holzmeister J; EchoCRT Study Group. Cardiac-resynchronization therapy in heart failure with a narrow QRS complex. *N Engl J Med*. 2013;369:1395–1405.
5. Perry R, De Pasquale CG, Chew DP, Aylward PE, Joseph MX. QRS duration alone misses cardiac dyssynchrony in a substantial proportion of patients with chronic heart failure. *J Am Soc Echocardiogr*. 2006;19:1257–1263.
6. Hor KN, Wansapura JP, Al-Khalidi HR, Gottliebson WM, Taylor MD, Czosek RJ, Nagueh SF, Akula N, Chung ES, Benson WD, Mazur W. Presence of mechanical dyssynchrony in Duchenne muscular dystrophy. *J Cardiovasc Magn Reson*. 2011;13:12.
7. Santos AB, Kraigher-Krainer E, Bello N, Claggett B, Zile MR, Pieske B, Voors AA, McMurray JJ, Packer M, Bransford T, Lefkowitz M, Shah AM, Solomon SD. Left ventricular dyssynchrony in patients with heart failure and preserved ejection fraction. *Eur Heart J*. 2014;35:42–47.
8. Mehta S, Asirvatham SJ. Rethinking QRS duration as an indication for CRT. *J Cardiovasc Electrophysiol*. 2012;23:169–171.
9. Kass DA. An epidemic of dyssynchrony: but what does it mean? *J Am Coll Cardiol*. 2008;51:12–17.
10. Rademakers LM, de Boeck BW, Maessen JG, Prinzen FW. Development of strategies for guiding cardiac resynchronization therapy. *Heart Fail Clin*. 2008;4:333–345.
11. Stavrakis S, Lazzara R, Thadani U. The benefit of cardiac resynchronization therapy and QRS duration: a meta-analysis. *J Cardiovasc Electrophysiol*. 2012;23:163–168.
12. Shah RM, Patel D, Molnar J, Ellenbogen KA, Koneru JN. Cardiac-resynchronization therapy in patients with systolic heart failure and QRS interval ≤130 ms: insights from a meta-analysis. *Europace*. 2015;17:267–273.

13. Lin Z, Pu WT. Strategies for cardiac regeneration and repair. *Sci Transl Med*. 2014;6:239rv1.
14. Matsa E, Sallam K, Wu JC. Cardiac stem cell biology: glimpse of the past, present, and future. *Circ Res*. 2014;114:21–27.
15. Nelson TJ, Martinez-Fernandez A, Terzic A. Induced pluripotent stem cells: developmental biology to regenerative medicine. *Nat Rev Cardiol*. 2010;7:700–710.
16. Zingman LV, Alekseev AE, Hodgson-Zingman DM, Terzic A. ATP-sensitive potassium channels: metabolic sensing and cardioprotection. *J Appl Physiol*. 2007;103:1888–1893.
17. Kane GC, Behfar A, Dyer RB, O'Cochlain DF, Liu XK, Hodgson DM, Reyes S, Miki T, Seino S, Terzic A. *KCNJ*11 gene knockout of the Kir6.2 K_{ATP} channel causes maladaptive remodeling and heart failure in hypertension. *Hum Mol Genet*. 2006;15:2285–2297.
18. Yamada S, Kane GC, Behfar A, Liu XK, Dyer RB, Faustino RS, Miki T, Seino S, Terzic A. Protection conferred by myocardial ATP-sensitive K^+ channels in pressure overload-induced congestive heart failure revealed in *KCNJ11* Kir6.2-null mutant. *J Physiol*. 2006;577:1053–1065.
19. Terzic A, Alekseev AE, Yamada S, Reyes S, Olson TM. Advances in cardiac ATP-sensitive K^+ channelopathies from molecules to populations. *Circ Arrhythm Electrophysiol*. 2011;4:577–585.
20. Nelson TJ, Martinez-Fernandez A, Yamada S, Perez-Terzic C, Ikeda Y, Terzic A. Repair of acute myocardial infarction by human stemness factors induced pluripotent stem cells. *Circulation*. 2009;120:408–416.
21. Nelson TJ, Martinez-Fernandez A, Yamada S, Mael AA, Terzic A, Ikeda Y. Induced pluripotent reprogramming from promiscuous human stemness related factors. *Clin Transl Sci*. 2009;2:118–126.
22. Yamada S, Arrell DK, Kane GC, Nelson TJ, Perez-Terzic CM, Behfar A, Purushothaman S, Prinzen FW, Auricchio A, Terzic A. Mechanical dyssynchrony precedes QRS widening in K_{ATP} channel-deficient dilated cardiomyopathy. *J Am Heart Assoc*. 2013;2:e000410 doi: 10.1161/JAHA.113.000410.
23. Behfar A, Yamada S, Crespo-Diaz R, Nesbitt JJ, Rowe LA, Perez-Terzic C, Gaussin V, Homsy C, Bartunek J, Terzic A. Guided cardiopoiesis enhances therapeutic benefit of bone marrow human mesenchymal stem cells in chronic myocardial infarction. *J Am Coll Cardiol*. 2010;56:721–734.
24. Recommendations for cardiac chamber quantification by echocardiography in adults: an update from the American Society of Echocardiography and the European Association of Cardiovascular Imaging. *J Am Soc Echocardiogr*. 2015;28:1–39.e14.
25. Indik JH, Pearson EC, Fried K, Woosley RL. Bazett and Fridericia QT correction formulas interfere with measurement of drug-induced changes in QT interval. *Heart Rhythm*. 2006;3:1003–1007.
26. Yamada S, Nelson TJ, Behfar A, Crespo-Diaz RJ, Fraidenraich D, Terzic A. Stem cell transplant into preimplantation embryo yields myocardial infarction-resistant adult phenotype. *Stem Cells*. 2009;27:1697–1705.
27. Schaper J, Meiser E, Stämmler G. Ultrastructural morphometric analysis of myocardium from dogs, rats, hamsters, mice, and from human hearts. *Circ Res*. 1985;56:377–391.
28. Schaper J, Froede R, Hein S, Buck A, Hashizume H, Speiser B, Friedl A, Bleese N. Impairment of the myocardial ultrastructure and changes of the cytoskeleton in dilated cardiomyopathy. *Circulation*. 1991;83:504–514.
29. Zlatkovic-Lindor J, Arrell DK, Yamada S, Nelson TJ, Terzic A. K_{ATP} channel-deficient dilated cardiomyopathy proteome remodeled by embryonic stem cell therapy. *Stem Cells*. 2010;28:1355–1367.
30. Arrell DK, Zlatkovic J, Kane GC, Yamada S, Terzic A. ATP-sensitive K^+ channel knockout induces cardiac proteome remodeling predictive of heart disease susceptibility. *J Proteome Res*. 2009;8:4823–4834.
31. 2013 ESC guidelines on cardiac pacing and cardiac resynchronization therapy: the task force on cardiac pacing and resynchronization therapy of the European Society of Cardiology. Developed in collaboration with the European Heart Rhythm Association. *Europace*. 2013;15:1070–1118.
32. Khazanie P, Hammill BG, Qualls LG, Fonarow GC, Hammill SC, Heidenreich PA, Al-Khatib SM, Piccini JP, Masoudi FA, Peterson PN, Curtis JP, Hernandez AF, Curtis LH. Clinical effectiveness of cardiac resynchronization therapy vs medical therapy alone among patients with heart failure: an analysis of the ICD and ADHERE National Registries. *Circ Heart Fail*. 2014;7:926–934.
33. Prinzen FW, Vernooy K, Auricchio A. Cardiac resynchronization therapy: state-of-the-art of current applications, guidelines, ongoing trials, and areas of controversy. *Circulation*. 2013;128:2407–2418.
34. Thibault B, Harel F, Ducharme A, White M, Ellenbogen KA, Frasure-Smith N, Roy D, Philippon F, Dorian P, Talajic M, Dubuc M, Guerra PG, Macle L, Rivard L, Andrade J, Khairy P; LESSER-EARTH Investigators. Cardiac resynchronization therapy in patients with heart failure and a QRS complex ≤120 milliseconds: the Evaluation of Resynchronization Therapy for Heart Failure (LESSER-EARTH) trial. *Circulation*. 2013;127:873–881.
35. Peterson PN, Greiner MA, Qualls LG, Al-Khatib SM, Curtis JP, Fonarow GC, Hammill SC, Heidenreich PA, Hammill BG, Piccini JP, Hernandez AF, Curtis LH, Masoudi FA. QRS duration, bundle-branch block morphology, and outcomes among older patients with heart failure receiving cardiac resynchronization therapy. *JAMA*. 2013;310:617–626.
36. Yancy CW, McMurray JJ. ECG—still the best for selecting patients for CRT. *N Engl J Med*. 2013;369:1463–1464.
37. Roberts A. Heart failure: CRT contraindicated in patients with short QRS duration. *Nat Rev Cardiol*. 2013;10:616.
38. Klemm HU, Krause KT, Ventura R, Schneider C, Aydin MA, Johnsen C, Boczor S, Meinertz T, Morillo CA, Kuck KH. Slow wall motion rather than electrical conduction delay underlies mechanical dyssynchrony in postinfarction patients with narrow QRS complex. *J Cardiovasc Electrophysiol*. 2010;21:70–77.
39. Yamada S, Terzic A. Reparative resynchronization in ischemic heart failure: an emerging strategy. *Expert Opin Biol Ther*. 2014;14:1055–1060.
40. Vernooy K, van Deursen CJ, Strik M, Prinzen FW. Strategies to improve cardiac resynchronization therapy. *Nat Rev Cardiol*. 2014;11:481–493.
41. Yamada S, Nelson TJ, Kane GC, Martinez-Fernandez A, Crespo-Diaz RJ, Ikeda Y, Perez-Terzic C, Terzic A. iPS cell intervention rescues ventricular wall motion disparity achieving biological cardiac resynchronization post-infarction. *J Physiol*. 2013;591:4335–4349.
42. Strik M, van Middendorp LB, Vernooy K. Animal models of dyssynchrony. *J Cardiovasc Transl Res*. 2012;5:135–145.
43. Mauritz C, Martens A, Rojas SV, Schnick T, Rathert C, Schecker N, Menke S, Glage S, Zweigerdt R, Haverich A, Martin U, Kutschka I. Induced pluripotent stem cell (iPSC)-derived Flk-1 progenitor cells engraft, differentiate, and improve heart function in a mouse model of acute myocardial infarction. *Eur Heart J*. 2011;32:2634–2641.
44. Sanchez-Freire V, Lee AS, Hu S, Abilez OJ, Liang P, Lan F, Huber BC, Ong SG, Hong WX, Huang M, Wu JC. Effect of human donor cell source on differentiation and function of cardiac induced pluripotent stem cells. *J Am Coll Cardiol*. 2014;64:436–448.
45. Kawamura M, Miyagawa S, Fukushima S, Saito A, Miki K, Ito E, Sougawa N, Kawamura T, Daimon T, Shimizu T, Okano T, Toda K, Sawa Y. Enhanced survival of transplanted human induced pluripotent stem cell-derived cardiomyocytes by the combination of cell sheets with the pedicled omental flap technique in a porcine heart. *Circulation*. 2013;128:S87–S94.
46. Lalit PA, Hei DJ, Raval AN, Kamp TJ. Induced pluripotent stem cells for post-myocardial infarction repair: remarkable opportunities and challenges. *Circ Res*. 2014;114:1328–1345.
47. Templin C, Zweigerdt R, Schwanke K, Olmer R, Ghadri JR, Emmert MY, Müller E, Küest SM, Cohrs S, Schibli R, Kronen P, Hilbe M, Reinisch A, Strunk D, Haverich A, Hoerstrup S, Lüscher TF, Kaufmann PA, Landmesser U, Martin U. Transplantation and tracking of human-induced pluripotent stem cells in a pig model of myocardial infarction: assessment of cell survival, engraftment, and distribution by hybrid single photon emission computed tomography/computed tomography of sodium iodide symporter transgene expression. *Circulation*. 2012;126:430–439.
48. Addis RC, Epstein JA. Induced regeneration—the progress and promise of direct reprogramming for heart repair. *Nat Med*. 2013;19:829–836.
49. Bijnens BH, Cikes M, Claus P, Sutherland GR. Velocity and deformation imaging for the assessment of myocardial dysfunction. *Eur J Echocardiogr*. 2009;10:216–226.
50. Kirk JA, Kass DA. Electromechanical dyssynchrony and resynchronization of the failing heart. *Circ Res*. 2013;113:765–776.
51. Cikes M, Sutherland GR, Anderson LJ, Bijnens BH. The role of echocardiographic deformation imaging in hypertrophic myopathies. *Nat Rev Cardiol*. 2010;7:384–396.
52. Bauer M, Cheng S, Jain M, Ngoy S, Theodoropoulos C, Trujillo A, Lin FC, Liao R. Echocardiographic speckle-tracking based strain imaging for rapid cardiovascular phenotyping in mice. *Circ Res*. 2011;108:908–916.
53. Cordero-Reyes AM, Youker K, Estep JD, Torre-Amione G, Nagueh SF. Molecular and cellular correlates of cardiac function in end-stage DCM: a study using speckle tracking echocardiography. *JACC Cardiovasc Imaging*. 2014;7:441–452.
54. Terzic A, Behfar A. Regenerative heart failure therapy headed for optimization. *Eur Heart J*. 2014;35:1231–1234.
55. Kramann R, Schneider RK, DiRocco DP, Machado F, Fleig S, Bondzie PA, Henderson JM, Ebert BL, Humphreys BD. Perivascular $gli1^+$ progenitors are key contributors to injury-induced organ fibrosis. *Cell Stem Cell*. 2015;16:51–66.

56. Forbes SJ, Rosenthal N. Preparing the ground for tissue regeneration: from mechanism to therapy. *Nat Med*. 2014;20:857–869.

57. Behfar A, Terzic A. Stem cells versus senescence: the yin and yang of cardiac health. *J Am Coll Cardiol*. 2015;65:148–150.

58. Kusunose K, Penn MS, Zhang Y, Cheng Y, Thomas JD, Marwick TH, Popović ZB. How similar are the mice to men? Between-species comparison of left ventricular mechanics using strain imaging. *PLoS One*. 2012;7:e40061.

59. Ogano M, Iwasaki YK, Tanabe J, Takagi H, Umemoto T, Hayashi M, Miyauchi Y, Shimizu W. Cardiac resynchronization therapy restored ventricular septal myocardial perfusion and enhanced ventricular remodeling in patients with nonischemic cardiomyopathy presenting with left bundle branch block. *Heart Rhythm*. 2014;11:836–841.